# Directional Droplet Transport and Fog Removal on Textured Surfaces Using Liquid Dielectrophoresis

Di Sun<sup>®</sup> and Karl F. Böhringer<sup>®</sup>, Fellow, IEEE

Abstract—This paper reports a droplet super-spreading and directional transport device using anisotropic ratchet conveyors (ARCs) and liquid dielectrophoresis (L-DEP). The ARC is created by patterning micro-sized hydrophilic curved rungs on a hydrophobic background. Micropatterning processes on the hydrophobic thin film have been successfully implemented by adopting a Parylene C stencil mask. The application of ARCs to transport the droplet using orthogonal vibrations to create self-cleaning surfaces was reported at the Hilton Head Workshop in 2018. The method presented in this paper utilizes interdigitated electrodes (IDE) to exert an L-DEP force on the droplet. By modulating the L-DEP force with an electromagnetic relay, the droplet can be directionally transported on the ARC-patterned surface independently of the droplet self-resonance frequency. The system works with a broad range of droplet volumes between 2  $\mu L$  and 20  $\mu$ L. The droplet can be transported with the presence of a moisture layer on the surface, which is superior to systems that move the droplet by relying on the solid-liquid interfacial tension difference like, e,g., in an electrowetting-on-dielectric (EWOD) system, since the moisture could block the solid-liquid interface and degrade the system ability to transport the droplet. This design also enables droplet manipulation in an open space configuration without a top cover plate, leading to a broad range of applications including self-cleaning surfaces and fog removal. [2020-0077]

Index Terms—Anisotropic ratchet conveyors, liquid dielectrophoresis, fog removal, parylene C.

Manuscript received April 19, 2020; revised May 24, 2020; accepted June 9, 2020. This research was funded in part by Amazon Catalyst, the University of Washington CoMotion Innovation Fund, and the National Science Foundation (grant number ECCS-1308025). Di Sun received support from the University of Washington NSF I-Corps site, a graduate fellowship from the UW Clean Energy Institute, and prizes from the Smukowski Family in the UW Business Plan Competition and from the Alaska Airlines Environmental Innovation Challenge. Part of this work was conducted at the Washington Nanofabrication Facility / Molecular Analysis Facility, a National Nanotechnology Coordinated Infrastructure (NNCI) site at the University of Washington, which was supported in part by funds from the National Science Foundation (grant numbers NNCI-1542101, 1337840 and 0335765), the National Institutes of Health, the Institute for Nano-engineered Systems, the Molecular Engineering & Sciences Institute, the Clean Energy Institute, the Washington Research Foundation, the M. J. Murdock Charitable Trust, Altatech, ClassOne Technology, GCE Market, Google, and SPTS. Subject Editor M. Rais-Zadeh. (Corresponding author: Karl F. Böhringer.)

Di Sun and Karl F. Böhringer are with the Department of Electrical and Computer Engineering, University of Washington, Seattle, WA 98195 USA, and also with the Institute for Nano-Engineered Systems, University of Washington, Seattle, WA 98195 USA (e-mail: dxs535@uw.edu; karlb@uw.edu).

Color versions of one or more of the figures in this article are available online at http://ieeexplore.ieee.org.

Digital Object Identifier 10.1109/JMEMS.2020.3001984

## I. INTRODUCTION

THE ability to remove microparticles or micro drops from ■ a surface is important for many applications, including self-cleaning surfaces [1]-[4], condensation heat transfer enhancement [5], [6] and anti-icing applications [7]. In the era of Internet of Things (IoT), robotics and autonomous vehicles (AV), it is crucial to keep the surface of optical sensors clean, like cameras or lidars, and to reduce the risk of malfunctioning and miscommunication [8]. Approaches have been proposed to actively or passively capture or counteract condensation and accelerate the speed of moisture removal from the surface. Walker et al. designed transparent light-absorbing metasurfaces using alternating thin layers of Au and TiO2 to reduce the defogging time under sun exposure [9]. Bai et al. [10] and Song and Bhushan [11] designed bio-inspired wettability gradient surfaces by creating hydrophilic wedge patterns on a hydrophobic or super-hydrophobic background to enable spontaneous water drop movement and improve the water collection efficiency. Yan et al. developed an enhanced water capture system taking advantage of the electrowetting-ondielectric (EWOD) effect [12].

In our manuscript, we performed an active surface cleaning approach for surface fog removal by a combination of anisotropic ratchet conveyors (ARCs) and liquid dielectrophoresis (L-DEP). ARCs consist of hydrophilic curved rungs on a hydrophobic background [13]. L-DEP agitates the droplet with interdigitated coplanar electrodes on an open surface configuration [14]–[16]. Anisotropic forces at the leading and trailing edges of the droplet directionally transport the droplet over each modulation cycle. The water condensation can be cleaned by the droplet transport along the ARC track.

## II. SYSTEM DESIGN

## A. Theory Background

Two electrohydrodynamic approaches have been widely applied to manipulate the water droplet wettability on a solid surface with an external electrical field, namely EWOD and L-DEP [17]. EWOD happens under DC or low AC frequencies (<1 kHz) with extra charge accumulating at the liquid-solid interface to alter the interfacial tension. L-DEP utilizes much higher frequencies ( $\sim$ 10 kHz - 200 kHz), and the polarization of the dipoles within the liquid gives rise to Maxwell stress at the liquid-air interface [18]. The L-DEP body force density acting on liquids can be expressed in terms of the

Korteweg-Helmholtz relation [19]:

$$\vec{f}_k = \sigma_f \vec{E} - \frac{\varepsilon_0}{2} E^2 \nabla \varepsilon_f + \nabla \left[ \frac{\varepsilon_0}{2} E^2 \frac{\delta \varepsilon_f}{\delta \rho} \rho \right]$$
 (1)

where  $\rho$  is the liquid density,  $\varepsilon_f$  is the liquid permittivity, E is the electrical field intensity, and  $\sigma_f$  is the free charge. The first term on the right describes the electrostatic force, the second term describes the dielectrophoresis force and the last term can be neglected because the fluid density remains constant. The penetration depth of the electrical potential, and thus the electrical field, decays exponentially from the liquid-solid interface into the liquid. The L-DEP force is strongest at the three-phase contact line. The motion of the liquid will be confined along the electrodes due to the periodic energy barriers.

#### B. Fabrication Process

The system was fabricated on Si wafers or glass substrates. The substrate was first cleaned with piranha solution (H<sub>2</sub>SO<sub>4</sub>:H<sub>2</sub>O<sub>2</sub> = 4 : 1) at 110 °C for 10 min, rinsed with deionized (DI) water and dried with nitrogen gas using a spin rinse dryer (Avenger Ultra-Pure, ClassOne Technology, Inc.). For the Si wafer, a layer of 2  $\mu$ m SiO<sub>2</sub> was deposited with PECVD (Delta LPX, SPTS Technologies, Inc.) at 350 °C as the substrate insulation layer. To fabricate the interdigitated electrodes (IDE), Cr thin film (100 nm) was deposited on the substrate by PVD sputtering (LAB 18, Kurt J. Lesker, Inc). Photoresist AZ1512 (1.2  $\mu$ m) was spin-coated on the wafer surface and the electrode ratchet pattern was directly exposed with a Heidelberg-MicroPG-101 mask writer (Heidelberg Instruments Mikrotechnik GmbH). The photoresist was developed with AZ340 photoresist developer (AZ340: DI water = 4:1) for 1 min. The IDE electrodes were etched by wet chemical processing using the Cr etchant for 2 min. SiN<sub>x</sub> thin film (350 nm) was deposited on top of the electrodes as the dielectric layer by a CVD process. Diluted Cytop (Asahi Glass Co. Ltd) was spin-coated on the dielectric layer and baked under 180 °C for 1 hour as the hydrophobic region. For Cytop patterning, we utilized Parylene C as a stencil mask since photoresist could not form a uniform layer on top of the hydrophobic Cytop surface [20]–[22]. Parylene C  $(2.5 \mu m)$  was evaporated on the Cytop using a commercial parylene coater (PDS 2010, Specialty Coating Systems, Inc.) under vacuum. Photoresist AZ9260 (6 µm) was coated and patterned. The Parylene C stencil mask and Cytop were etched through together with O2 plasma using reactive ion etching (Vision 320 RIE, Plasma-Therm, Inc.). The Parylene C stencil mask was peeled off with tweezers. The exposed SiN<sub>x</sub> regions without the Cytop coverage was treated with spin-on hexamethyldisilazane (HMDS) for a hydrophilic surface finish. The whole wafer was baked at 110 °C for 2 min to improve the bonding of the HMDS to the SiN<sub>x</sub> regions.

## C. Experimental Setup

AC signals were provided by a function generator (33120A, Agilent Inc.) and amplified by a voltage amplifier (PZD700, Trek Co.) with an amplifying factor of 200 V/V. A water

droplet was pipetted, and the droplet silhouette was monitored by a high-speed camera (FASTCAM Mini UX100) with a sampling rate of 1000 fps. The droplet edge and contact angle change with time were analyzed with MATLAB custom-made code. The function generator and high-speed camera were synchronized by a transistor-transistor logic (TTL) input port to capture the droplet shape change with time under the electrical field. To transport the droplet, an Arduino compatible electromagnetic relay board was controlled by a digital signal that turned on and off the electrical voltage applied to the IDE. The water droplet static contact angle (CA) on uniformly coated Cytop surfaces was measured with a Krüss Drop Shape Analyzer (DSA 100). For the droplet sliding angle measurement, a custom-made experimental setup was designed using a 3-axis accelerometer (MMA8451 from Adafruit).

## III. CHARACTERIZATION RESULTS

We first tested 3 different IDE electrode designs with a layer of uniform Cytop coating for the study of droplet spreading width and contact angle under a high frequency square wave input signal. The non-uniform electric fringe field-induced dipoles in liquid resulted in the L-DEP force on the droplet. The L-DEP force was sensitive to the input voltage and frequency [23]–[25]. The steady-state droplet width under different frequencies is plotted in Fig 1. It follows from equation (1) that for deionized water,  $\sigma_f$  is close to zero and the L-DEP body force becomes  $\vec{f}_k = -\frac{\varepsilon_0}{2} E^2 \nabla \varepsilon_f$ . A larger AC voltage amplitude input led to a stronger E-field and a stronger L-DEP body force. At the same time, the dielectric constant of water was dependent on the input frequency and thus influenced the magnitude of the L-DEP body force. A stronger L-DEP body force resulted in more droplet deformation and contact angle change. Compared with the interdigitated straight-line design electrodes, the folded-line design electrodes helped the droplet to overcome the periodic energy barriers and spread wider. The maximum droplet width under L-DEP could be more than twice compared to the initial droplet width on the Cytop surface with zero voltage input.

Fig. 2 shows the droplet contact angle change under different voltage amplitudes on the straight-line IDE electrodes. The voltage ranged between 0 and 360 V. As the input voltage increased within the tested range, the droplet spread along the longitudinal finger electrodes and the contact angle decreased from 108° to 38°, demonstrating a strong wetting and super-spreading behavior of the droplet under L-DEP force, which was impossible to achieve using an electrowetting-on-dielectric (EWOD) platform. Our previous measurements showed that the contact angle under DC voltage only varied between 108° and 80° [20]. The droplet contact angle stopped to further decrease because of the contact angle saturation [26].

We then patterned hydrophilic (arc central angle of 120°) ARC rungs on Cytop using the Parylene C stencil mask process. Fig. 3(a) shows an example of the ARC patterns on top of the IDE and dielectric layers. The center line of the ARC pattern was parallel to the longitudinal IDE finger directions. As shown in Fig. 3(b), the Cytop maintained good

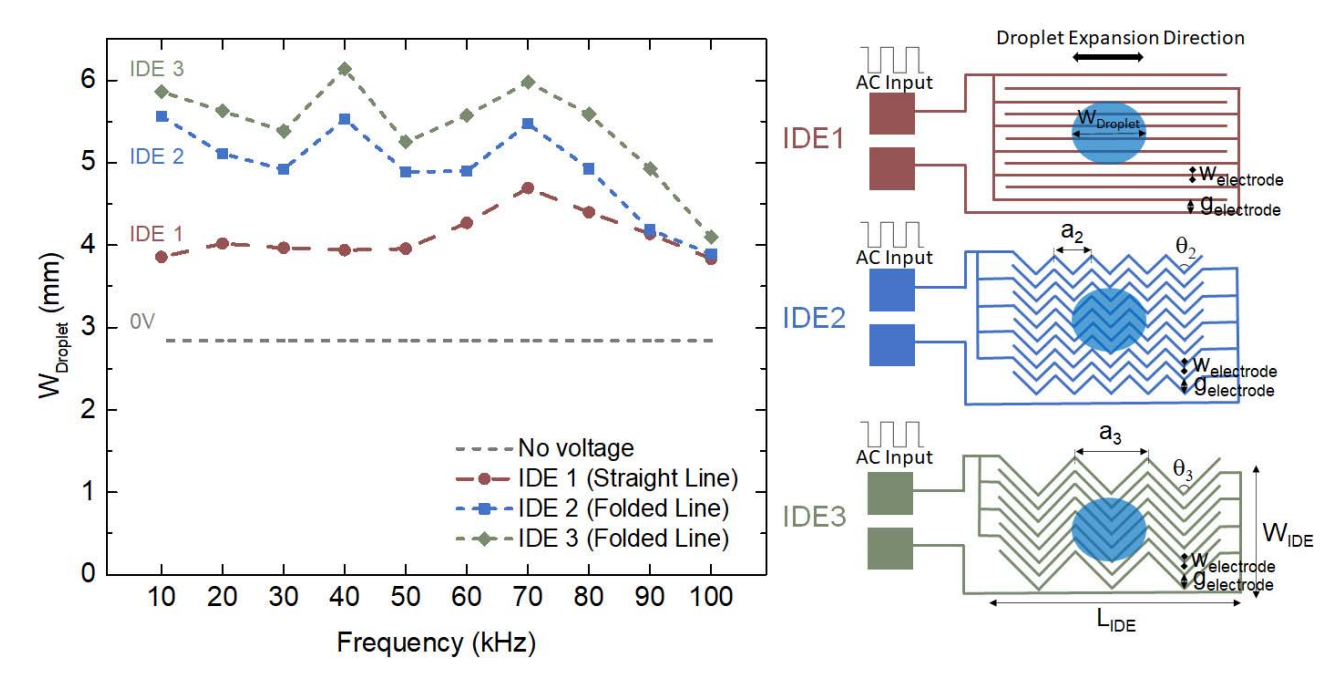


Fig. 1. Droplet (10  $\mu$ L) width in steady state in response to the AC square wave input frequency. The AC voltage amplitude is 400 V<sub>pp</sub>. The frequency varies from 10 kHz to 100 kHz. We investigated 3 designs of the IDE electrodes with a straight line design and two folded line designs. The gap between adjacent electrodes ( $g_{electrode}$ ) is 50  $\mu$ m. The width of each single electrode ( $g_{electrode}$ ) is 50  $\mu$ m. The total length of the IDEs ( $g_{IDE}$ ) is 12.5 mm. The total width of the IDEs ( $g_{IDE}$ ) is 5 mm. For the folded line design,  $g_{IDE}$ 0 mm and  $g_{IDE}$ 1 mm,  $g_{IDE}$ 2 mm and  $g_{IDE}$ 3 mm.

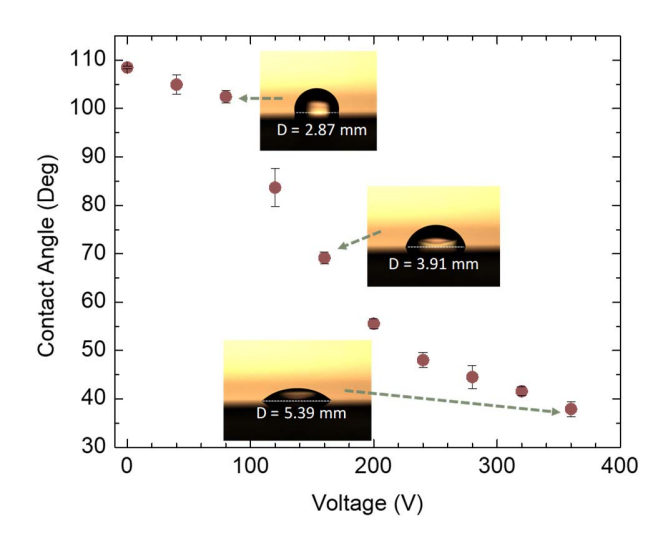


Fig. 2. Droplet (10  $\mu$ L) contact angle change vs. AC square wave voltage amplitude. The AC square wave voltage has a frequency of 10 kHz. Data is shown with  $\pm$  one standard deviation for n = 3 different measurements.

hydrophobicity with a high contact angle and a low sliding angle after peeling off Parylene C when compared with the Cytop surface as deposited. Fig. 3(c) shows the configuration setup to control the droplet to move on the ARC patterned surface using L-DEP force. The function generator continuously output the AC square voltage, which was amplified by a voltage amplifier. With the assistance of the ARC pattern, we were able to directionally move the droplet by modulating the input AC voltage with an electromagnetic relay. The relay was turned on and off with the Arduino microcontroller so that the droplet would expand and recess periodically along the

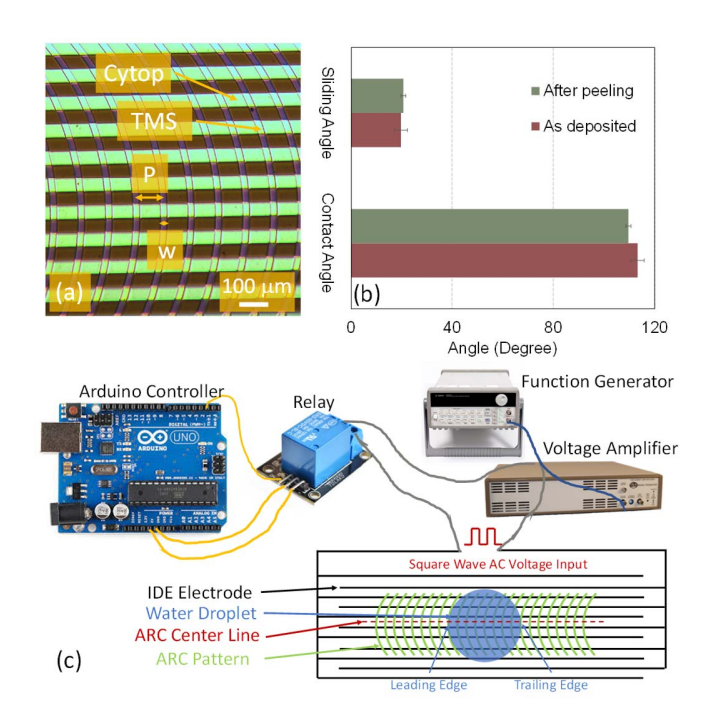


Fig. 3. (a) Microscope image of ARC patterns on Cytop. For each curved rung, the radius of curvature (R) is 1000  $\mu m$ , the etched linewidth (w) is 10  $\mu m$ , and the period (P) between adjacent rung centers is 100  $\mu m$ . (b) Contact angle and sliding angle measurement for Cytop before and after peeling off Parylene C. (c) Schematic of the test setup and ARC patterned surface.

ARC pattern. The droplet then transported along the surface with the help of anisotropic forces at the leading and trailing edge during each cycle [20].

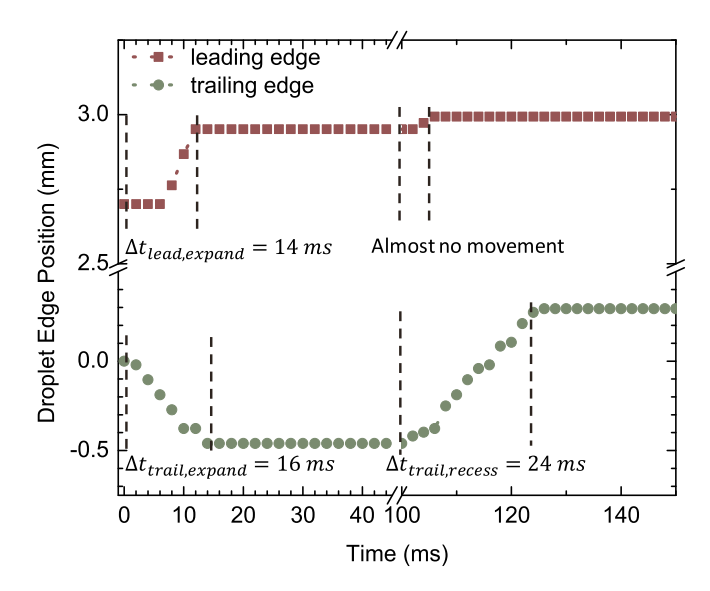


Fig. 4. Droplet (10  $\mu$ L) edge position change with time during expansion and recession phase. The AC voltage is 300 V<sub>pp</sub> at a frequency of 10 kHz. The AC voltage is modulated by the electromagnetic relay every 100 ms to connect or disconnect with the IDE electrode.

Fig. 4 shows the characterization results of the droplet leading and trailing edge position change and spreading time. The AC square voltage was turned on and off every 100 ms (5 Hz modulation frequency). During the expansion phase, when the AC square voltage was connected, the leading edge expanded by 290  $\mu$ m within 14 ms and the trailing edge expanded by 460  $\mu$ m within 16 ms. During the recession phase, when the AC square voltage was disconnected, the leading edge was pinned by the ARC pattern with little movement while the trailing edge recessed at 750  $\mu$ m within 24 ms. The average movement distance during each modulation cycle was about 290  $\mu$ m. The total time spent on the droplet expansion and recession was 40 ms, thus the potentially fastest modulation frequency was 25 Hz, and the potentially fastest droplet transport speed under this condition was estimated at the order of 7.25 mm/s.

Fig. 5 shows a top view demonstration of the droplet transport by our L-DEP platform with the assist of ARCs. Compared with the mechanically driven system [1], the L-DEP platform could transport the droplet independently of the droplet self-resonance frequency while using only two control terminals without complex control circuitry. In the mechanically driven system, the external drive frequency was chosen to match the sessile droplet resonance frequency (at the order of tens of Hz) in order to achieve the maximum expansion amplitude. The droplet expansion amplitude rapidly decayed as the mechanical drive frequency deviated from the droplet resonance frequency and the droplet stopped moving. In contrast, on the L-DEP platform, the droplet's maximum expansion was tuned by the external electrostatic field. The longitudinal length of the IDE electrodes was 20 mm and the total width was 6.4 mm. The ARC track was patterned at the center of the IDE electrodes. We also tested different droplet sizes on the same ARC track design and droplets from  $2 \mu L$  to  $20 \mu L$  could be transported along. The current drawn

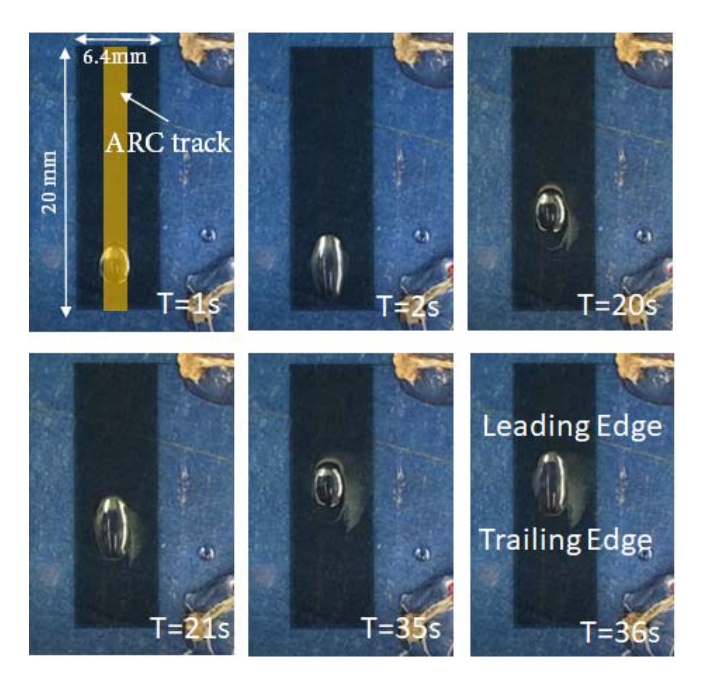


Fig. 5. Top view of a 10  $\mu$ L droplet moving on the IDE electrodes with ARC patterns. The electromagnetic relay was switched on and off every 1 s. The AC voltage was 400 V<sub>pp</sub> at 20 kHz. The average transport speed was estimated as 0.17 mm/s. The patterned ARC track region is highlighted in yellow shading in the T=1s figure.

from the voltage amplifier was measured at a peak-to-peak level of 11 mA under a 400  $V_{pp}$  actuation voltage at 20 kHz. The current consumption when the droplet rested on ARC patterns increased  $\sim\!2.6\%$  when compared with the droplet resting on the uniform Cytop surface.

We exposed our device surface to a humidifier for at least 60 seconds to cover the entire device surface with tiny drops that mimic a foggy surface. The drop sizes on the surface ranged between  $1\sim100~\mu m$  in diameter based on image processing with ImageJ software. The estimated thickness was in the order of tens of microns on average. Then we pipetted a droplet on the ARC track and turned on the AC voltage input. As evident from the sequential images in Fig. 6, the droplet was able to move along the ARC track and clean the fog away. Fig. 6 (a) shows the initial state when the droplet was put on the foggy surface and Fig. 6 (b)-(f) present the droplet when it was actuated. We noticed that the external voltage helped in the merging of the tiny drops to larger ones before the surface was further cleaned by the 10  $\mu$ L droplet. The L-DEP force could still deform the droplet in the presence of multiple tiny water drops on the surface. This behavior is different from the EWOD system, where the droplet would stop moving or reduce its moving speed when a layer of fog is present, since the fog layer blocks the solid-liquid interface. The system was only tested with fog generated from DI water. We believe that our system could remove fog with low conductivity (<1 mS/m), while a modified design in terms of dielectric materials and electrode geometry optimization would be necessary for more conductive solutions (in the order of 10 mS/m) [27].

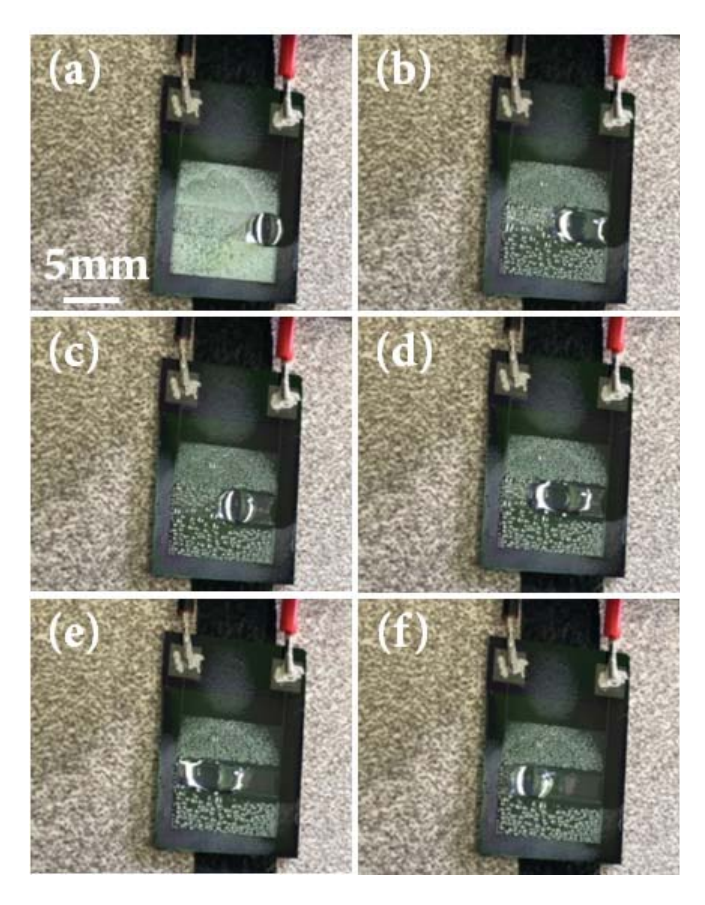


Fig. 6. (a)-(f) sequential images of surface fog removal using a 10  $\mu L$  droplet.

## IV. CONCLUSION

In this paper, we presented the design, fabrication, and characterization of droplet transport with L-DEP on an ARC track. The system demonstrated the robust capability to transport a broad range of droplet sizes and to manipulate the droplet independently of resonance frequencies for different volumes. The setup required an electromagnetic relay to modulate the high input voltages but no additional complex control circuitry. We predicted that the droplet could be moved at a speed of 7.25 mm/s based on the droplet response time during expansion and recession. We also presented the capability to remove surface fog with our design, which has proven difficult to accomplish with an EWOD system.

As for future plans, we will explore the influence of IDE line width and gap size on the droplet manipulation and fog removal. We will also experiment with different ARC designs to transport and collect smaller droplets with less than  $100~\mu m$  diameter. Our ultimate goal is to perform fog removal without the aid of a manually dispensed cleaning droplet.

#### REFERENCES

- D. Sun and K. F. Böhringer, "Active self-cleaning surfaces on solar modules," in *Proc. Hilton Head Workshop, Solid-State Sens.*, Actuators Microsyst. Workshop, Hilton Head Island, SC, USA, 2018, pp. 261–264.
- [2] K. Zhang, Z. Li, M. Maxey, S. Chen, and G. E. Karniadakis, "Self-cleaning of hydrophobic rough surfaces by coalescence-induced wetting transition," *Langmuir*, vol. 35, no. 6, pp. 2431–2442, Feb. 2019.

- [3] T. Heckenthaler, S. Sadhujan, Y. Morgenstern, P. Natarajan, M. Bashouti, and Y. Kaufman, "Self-cleaning mechanism: Why nanotexture and hydrophobicity matter," *Langmuir*, vol. 35, no. 48, pp. 15526–15534, Dec. 2019.
- [4] D. Sun and K. Böhringer, "Self-cleaning: From bio-inspired surface modification to MEMS/microfluidics system integration," *Microma-chines*, vol. 10, no. 2, p. 101, Jan. 2019.
- [5] N. Miljkovic, D. J. Preston, R. Enright, and E. N. Wang, "Electrostatic charging of jumping droplets," *Nature Commun.*, vol. 4, no. 1, pp. 1–9, Dec. 2013.
- [6] N. Miljkovic *et al.*, "Jumping-droplet-enhanced condensation on scalable superhydrophobic nanostructured surfaces," *Nano Lett.*, vol. 13, no. 1, pp. 179–187, Jan. 2013.
- [7] T.-S. Wong *et al.*, "Bioinspired self-repairing slippery surfaces with pressure-stable omniphobicity," *Nature*, vol. 477, no. 7365, pp. 443–447, Sep. 2011.
- [8] K. Y. Lee, J. Hong, and S. K. Chung, "Smart self-cleaning lens cover for miniature cameras of automobiles," *Sens. Actuators B, Chem.*, vol. 239, pp. 754–758, Feb. 2017.
- [9] C. Walker, E. Mitridis, T. Kreiner, H. Eghlidi, T. M. Schutzius, and D. Poulikakos, "Transparent metasurfaces counteracting fogging by harnessing sunlight," *Nano Lett.*, vol. 19, no. 3, pp. 1595–1604, Mar. 2019.
- [10] H. Bai, L. Wang, J. Ju, R. Sun, Y. Zheng, and L. Jiang, "Efficient water collection on integrative bioinspired surfaces with star-shaped wettability patterns," *Adv. Mater.*, vol. 26, no. 29, pp. 5025–5030, Aug. 2014.
- [11] D. Song and B. Bhushan, "Optimization of bioinspired triangular patterns for water condensation and transport," *Phil. Trans. Roy. Soc. A*, *Math., Phys. Eng. Sci.*, vol. 377, no. 2150, Jul. 2019, Art. no. 20190127.
- [12] R. Yan et al., "Enhanced water capture induced with electrowetting-on-dielectric (EWOD) approach," Appl. Phys. Lett., vol. 113, no. 20, Nov. 2018, Art. no. 204101.
- [13] T. A. Duncombe, J. F. Parsons, and K. F. Böhringer, "Directed drop transport rectified from orthogonal vibrations via a flat wetting barrier ratchet," *Langmuir*, vol. 28, no. 38, pp. 13765–13770, Sep. 2012.
- [14] G. McHale, C. V. Brown, and N. Sampara, "Voltage-induced spreading and superspreading of liquids," *Nature Commun.*, vol. 4, no. 1, pp. 1–7, Jun. 2013.
- [15] G. McHale, C. V. Brown, M. I. Newton, G. G. Wells, and N. Sampara, "Dielectrowetting driven spreading of droplets," *Phys. Rev. Lett.*, vol. 107, no. 18, Oct. 2011, Art. no. 186101.
- [16] R. Ahmed, D. Hsu, C. Bailey, and T. Jones, "Dispensing picoliter droplets using dielectrophoretic (DEP) microactuation," *Microscale Thermophys. Eng.*, vol. 8, no. 3, pp. 271–283, 2004.
- [17] A. M. J. Edwards, C. V. Brown, M. I. Newton, and G. McHale, "Dielectrowetting: The past, present and future," *Current Opinion Colloid Interface Sci.*, vol. 36, pp. 28–36, Jul. 2018.
- [18] T. B. Jones, J. D. Fowler, Y. S. Chang, and C.-J. Kim, "Frequency-based relationship of electrowetting and dielectrophoretic liquid microactuation," *Langmuir*, vol. 19, no. 18, pp. 7646–7651, Sep. 2003.
- [19] J. Berthier and K. A. Brakke, The Physics of Microdroplets. Hoboken, NJ, USA: Wiley, 2012.
- [20] D. Sun and K. F. Böhringer, "EWOD-aided droplet transport on texture ratchets," Appl. Phys. Lett., vol. 116, no. 9, Mar. 2020, Art. no. 093702.
- [21] D. Sun and K. F. Böhringer, "Photovoltaic module active self-cleaning surface using anisotropic ratchet conveyors fabricated with parylene-C stencil," *J. Phys., Conf. Ser.*, vol. 1052, Jul. 2018, Art. no. 012014.
- [22] D. Sun and K. F. Bohringer, "Self-cleaning surfaces using anisotropic ratchet conveyors," in *Proc. 19th Int. Conf. Solid-State Sens.*, Actuators Microsyst. (TRANSDUCERS), Jun. 2017, pp. 1773–1776.
- [23] H. Geng, J. Feng, L. M. Stabryla, and S. K. Cho, "Dielectrowetting manipulation for digital microfluidics: Creating, transporting, splitting, and merging of droplets," *Lab Chip*, vol. 17, no. 6, pp. 1060–1068, 2017.
- [24] T. B. Jones, K.-L. Wang, and D.-J. Yao, "Frequency-dependent electromechanics of aqueous liquids: Electrowetting and dielectrophoresis," *Langmuir*, vol. 20, no. 7, pp. 2813–2818, Mar. 2004.
- [25] C.-H. Chen, S.-L. Tsai, M.-K. Chen, and L.-S. Jang, "Effects of gap height, applied frequency, and fluid conductivity on minimum actuation voltage of electrowetting-on-dielectric and liquid dielectrophoresis," *Sens. Actuators B, Chem.*, vol. 159, no. 1, pp. 321–327, Nov. 2011.
- [26] A. Quinn, R. Sedev, and J. Ralston, "Contact angle saturation in electrowetting," J. Phys. Chem. B, vol. 109, no. 13, pp. 6268–6275, Apr. 2005.
- [27] R. Renaudot et al., "Optimized micro devices for liquiddielectrophoresis (LDEP) actuation of conductive solutions," Sens. Actuators B, Chem., vol. 177, pp. 620–626, Feb. 2013.



Di Sun received the B.Eng. degree from the Department of Electrical Engineering and Automation, Xi'an Jiaotong University, Xi'an, Shaanxi, China, in 2011, and the M.Sc. degree from the Department of Electrical Engineering and Computer Science, Case Western Reserve University, Cleveland, OH, USA, in 2014. He is currently pursuing the Ph.D. degree with the Prof. Karl F. Böhringer's MEMS Laboratory, Department of Electrical and Computer Engineering, University of Washington, Seattle, WA, USA.

He has research experience in MEMS/microfludics for self-cleaning surfaces and lab-on-chip applications, implantable MEMS packaging and soft electronics for human-computer interactions. He had multiple internship experiences, including a Failure Analysis Engineer at Pixtronix, Andover, MA, USA, a Process Engineer at Lam Research, Tualatin, OR, USA, and Fluke, Everett, WA, USA, a Research Engineer at Microsoft, Redmond, WA, USA, and a Process Integration Engineer at OmniVision, Santa Clara, CA, USA. He will be joining Microsoft's HoloLens Group (Redmond, WA) as an Optical Engineer.

Mr. Sun serves as the Student Fellow for the Clean Energy Institute (CEI), University of Washington. He also serves as the Student Torrance Tech Due Diligence Analyst for E8 Angles, Seattle, WA, USA.



**Karl F. Böhringer** (Fellow, IEEE) received the Dipl.Inform. degree from the University of Karlsruhe, Germany, in 1990, and the M.S./Ph.D. degrees in computer science from Cornell University, Ithaca, NY, USA, in 1993 and 1997, respectively.

He was a Visiting Scholar with Stanford University from 1994 to 1995 and a Postdoctoral Researcher with the University of California, Berkeley, from 1996 to 1998. He joined the University of Washington, Seattle, WA, USA, in 1998, where he is currently a Professor of electrical and computer

engineering and bioengineering, the Director of the Nano-engineered Systems Institute, and a Site Director of the University of Washington and Oregon State University node in the NSF National Nanotechnology Infrastructure Network. He held visiting positions at the Universities of Tohoku, Tokyo, Kyoto, Japan, São Paulo, Brazil, and the École Polytechnique Fédérale de Lausanne, Switzerland. He is a Co-Founder of Tunoptix, a University of Washington spin-off developing tunable metasurface optics for machine vision and AR/VR applications. His awards include the John M. Fluke Distinguished Chair of Engineering, University of Washington in 2010, the Invitational Fellowship for Research in Japan by the Japan Society for the Promotion of Science (JSPS) in 2004, the IEEE Robotics and Automation Society Academic Early Career Award in 2004, the NSF CAREER Award in 1999, and the NSF Postdoctoral Associateship in 1997. His work was listed among the Top 100 Science Stories of 2002 in Discover magazine. He has served as an Editor for ASME/IEEE JOURNAL OF MICROELECTROMECHANICAL SYSTEMS, the IEEE TRANSACTIONS ON AUTOMATION SCIENCE AND ENGINEERING, Frontiers in Mechanical Engineering, and Microsystems and Nanoengineering (Nature Publishing Group). He has served among others, on the technical program committees for the IEEE International Conference on Microelectromechanical Systems (MEMS) and the International Conference Solid-State Sensors, Actuators and Microsystems (Transducers) conferences, He was a General Co-Chair of the IEEE MEMS in 2011.